Mössbauer Studies for Exploring CMR and TMR Perovskites

Z. Németh[a,c,*], Z. Klencsár[b], A. Vértes[a], and K. Nomura[c,*]

[a]*Laboratory of Nuclear Chemistry, Institute of Chemistry, Eötvös Loránd University and Chemical Research Center, Hungarian Academy of Sciences, Pázmány P. s. 1/A, Budapest, Hungary*
[b]*Department of Surface Modifications and Nanostructures, Chemical Research Center, Hungarian Academy of Sciences, Pusztaszeri út 59-67, Budapest, 1025, Hungary*
[c]*School of Engineering, The University of Tokyo, 7-3-1 Hongo, Bunkyo-ku, Tokyo 113-8656, Japan*

In the present review we show a series of recent studies with the aim of exploring the electronic and magnetic structure of materials with perovskite structure and strong magnetoresistance effect. The examined samples include $Sr_{2-x}A_xFeMO_6$ (A = Ca, Ba and M = Mo, Re, Ru) double perovskites with $x = 0$ and 0.1 and iron doped $La_{0.8}Sr_{0.2}Fe_yCo_{1-y}O_{3-\delta}$ cobaltate perovskites with $0 \leq y \leq 0.3$. Besides understanding the basic electronic and magnetic interactions presented by these compounds, we have tried to trace nanoscale phase separation, which has been introduced as a key feature for both colossal and intrinsic tunneling magnetoresistance recently.

1. Introduction

Doped transition metal compounds with complex electronic and magnetic structures show a wide range of new physical phenomena like high-temperature superconductivity, room temperature magnetic semiconductivity, or colossal magnetoresistance (CMR).[1-3] Following the discovery of the effect of colossal negative magnetoresistance in manganese based perovskites,[4-7] several different classes of transition metal compounds such as Sr_2FeMoO_6 double perovskites[8] or $La_{1-x}Sr_xCoO_3$ perovskites[9-12] were found to exhibit unusually high magnetoresistance (MR) partly as a peak around their Curie-temperature (CMR effect), partly as an increasing feature with decreasing temperature (tunneling-type magnetoresistance, TMR)(Table1). The most important difference between these two types of MR is their temperature dependence: while CMR effect manifests

only around the magnetic temperature as a peak in the MR *vs.* T plot, TMR increases monotonically with decreasing temperature. Due to the complexity of the underlying physical and chemical processes in these materials, the understanding of their electronic and magnetic structure is one of the most vital topics in condensed matter physics nowadays.

The first models aiming to shed light on the CMR effect found in manganite perovskites, and to explain the unusually strong correlation between the magnetic state of the material and its electric transport properties were based on the theories of double exchange model[13] and strong electron-lattice interactions.[14] The former was based on the fact that in $La_{1-x}Ca_xMnO_3$ perovskites the doping divalent ions (usually Ca) introduce a number of x extra electrons to the system, either oxidizing Mn^{3+} ions into Mn^{4+} or creating oxygen vacancies, although for low doping rates the latter effect was found to be negligible. As a

TABLE 1: Magnetoresistance of perovskites and double perovskites of different composition

Chemical formula	Doping level	TMR at RT	CMR at T_m	TMR ≤ 10 K	Ref.
$La_{0.75}Ca_{0.25}MnO_3$		-	80%	40%	(6)
$La_{0.63}Ca_{0.37}Fe_xMn_{1-x}O_3$	$x = 0.12$	-	99.75%	99.9%	(7)
$La_{0.8}Sr_{0.2}Fe_xCo_{1-x}O_{3-\delta}$	$x = 0$	-	6%	13%	(78)
	$x = 0.025$	-	8%	84%	(79)
	$x = 0.05$	-	9%	71%	(80)
	$x = 0.15$	-	-	37%	(81)
	$x = 0.2$	-	-	29%	(81)
	$x = 0.3$	-	-	10%	(81)
Sr_2FeMoO_6		5%	-	42%	(8)
$Sr_{2-x}Ca_xFeMoO_6$	$x = 0.1$	11%	-	?	(39)
$Sr_{2-x}Ba_xFeMoO_6$	$x = 1.6$	11%	-	?	(39)
Sr_2FeReO_6		7%	-	21%	(26)
Sr_2FeCoO_6		-	-	15%	(48)
Sr_2FeRuO_6		1%	-	25%[*]	(59)

[*] Measured at 110 K

*Corresponding author. E-mail: hentes@chem.elte.hu, k-nomura@t-adm.t.u-tokyo.ac.jp

result, beside the Mn^{3+}–Mn^{3+} antiferromagnetic superexchange interactions, Mn^{3+}–Mn^{4+} ferromagnetic coupling manifests due to electrons being itinerant between the manganese ions. It was shown that for a pair of cations two electrons move at the same time, one from the trivalent manganese to the intermediate oxygen, while the other from the oxygen to the Mn^{4+} (hence the name double exchange). This phenomenon (in contrast with super exchange) requires the ferromagnetic ordering of the transition metal ions, so the ferromagnetism and the itinerancy of the electrons are strongly correlated.[13] Later on, it was suggested that an unusually strong effect of the distortion of the crystal lattice on the local trapping of electrons should be taken into consideration, as well.[14] However, a high number of compounds were found to show CMR effect, which has neither double exchange nor Jahn-Teller distortions, which made the necessity of these phenomena for the realization of colossal magnetoresistance doubtful.[2]

Recently it was suggested that the doping at the rare earth site in these materials can lead to electronic phase separation, which is essential in the appearance of the CMR effect.[2,15,16] This phase separation in manganese perovskites was attributed to the locally increased density of Mn^{4+} ions in Sr rich regions, and so the local occurrence of the double exchange effect. It is worth to express that the exact meaning of the term 'local' used here is still debated, ranging from few tens of nanometers to micrometers.[17-20] This model suggests that magnetic clusters form even just above the magnetic ordering temperature (T_m), where they cannot build up long range magnetic order. However, an external magnetic field (H_{ext}) can have a huge effect on enhancing the long range magnetism at this small temperature range. As magnetism and electric conductivity are connected to each other strongly in CMR materials, the appearance of bulk magnetism above T_m due to the external magnetic field results in a colossal increase of bulk conductivity, which is the magnetoresistance effect (Figure 1).

The tunneling type magnetoresistance is usually explained by the polarization dependent hopping of electrons between magnetically ordered regions. In a simplified picture, the probability of electron transfer between ferromagnetically ordered areas is the highest if the magnetization of the two clusters is aligned. However, spin glass like systems, where the magnetic regions are connected via several different magnetic interactions, are in a frustrated state with randomly aligned magnetizations. An external magnetic field can influence this alignment to enhance the electron hopping, if the distance between the conducting regions is small enough. The lower the temperature, the higher the effect of H_{ext}, *i.e.* the higher the TMR ratio. This theory requires either a magnetic phase separation (as in the case of CMR effect) or a TMR effect between crystal grains (Figure 2).

It follows then that the close investigation of the electronic and magnetic phase separation phenomenon seems to be the key point in the study of peculiar magnetoresistance effects. In this review we show some recent studies on perovskite structured CMR and TMR materials concerning their electronic and magnetic structure. Besides the numerous bulk investigation techniques, applying Mössbauer spectrometry gives a unique possibility to discover the local state of iron, and to distinguish between electronically dissimilar regions even on a nanometer scale.

2. $Sr_{2-x}A_xFeMO_6$ (*A* = Ca, Ba and *M* = Mo, Re, Ru) double perovskites with *x* = 0, 0.1

Double perovskite systems consist of divalent cations in the first crystallographic site and two transition metal ions occupying alternatively the other metal sites of the perovskite structure (Figure 3). The two transition metal elements are usually high spin 3d and low spin 4d or 5d atoms. In principle, the
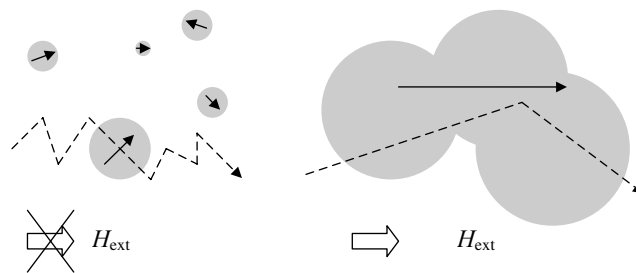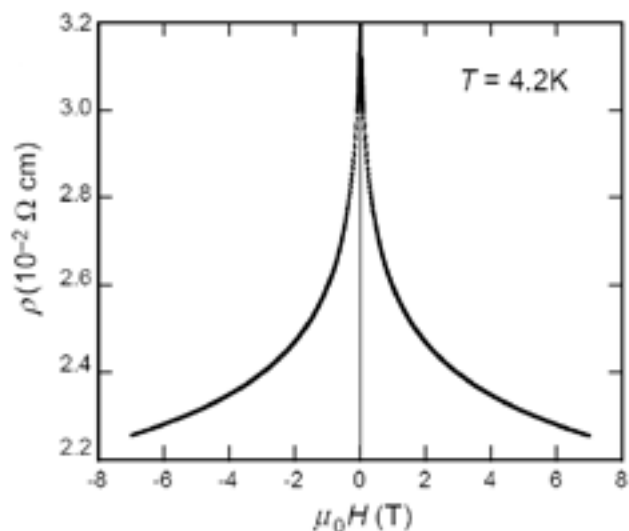

Figure 1. Schematic draw of the phase separation based theory of colossal magnetoresistance. The grey areas represent magnetically ordered clusters with an arrow indicating their magnetization. The dashed arrows symbolize the path of electrons. The more scattered the path, the less the electric conductivity. The white arrows indicate the absence or presence of external magnetic field. The left panel shows the magnetic state above the bulk magnetic ordering temperature with some small magnetic clusters in a nonmagnetic matrix in the absence of an external magnetic field (H_{ext}). The right panel shows the effect of H_{ext}: the magnetic clusters grow to coalesce, which results in the increase of bulk electric conductivity.
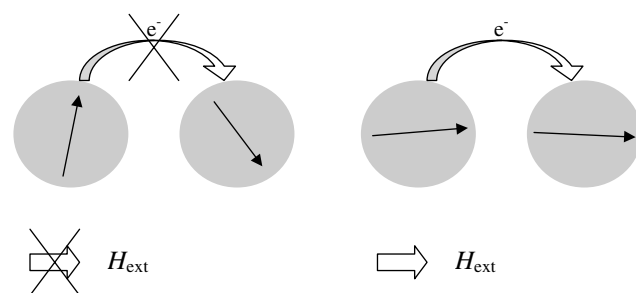
Figure 2. Schematic picturing of the phase separation based theory of tunneling type magnetoresistance. The grey areas represent magnetically ordered clusters with an arrow indicating their magnetization. The white arrows indicate the absence or presence of external magnetic field. The left panel shows the glassy magnetic state with the frozen magnetization vectors of magnetic clusters in the absence of an external magnetic field (H_{ext}). The right panel shows the effect of H_{ext}: the magnetization of magnetic clusters tend to align with H_{ext}, making the electron hopping more probable and thus increase bulk electric conductivity.
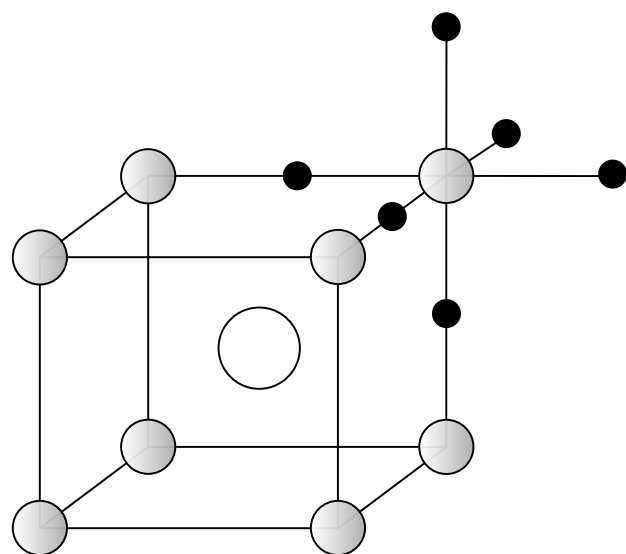
Figure 3. Scheme of the basic ABO_3 perovskite structure. In a cubic cell representation the A cations occupy the center of the cube (white sphere), while the B cations are on the corners (grey spheres). Oxygen atoms (black spheres), surrounding octahedral the B ions, are only indicated for one B. In a double perovskite, B sites are filled alternatively (by *e.g.* with Fe and Mo).
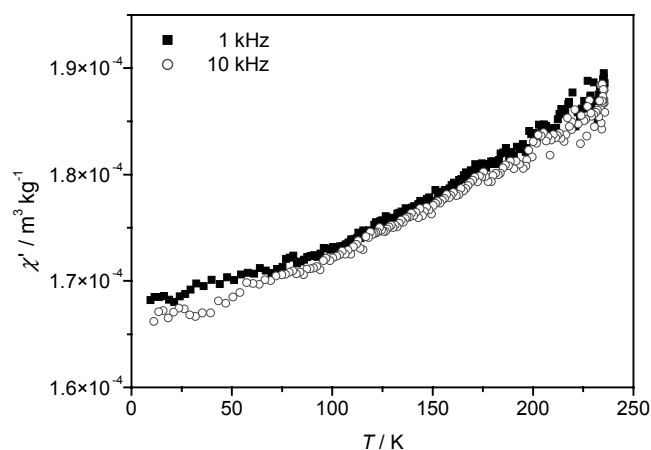
Figure 4. Magnetoresistance of Sr_2FeMoO_6 at 4.2 K. Figure taken from Reference 8.

Figure 5. AC magnetic susceptibility of Sr_2FeMoO_6 recorded with different frequencies.

Figure 6. ^{57}Fe Mössbauer spectra of Sr_2FeMoO_6 at 300 K and 4.2 K. While one of the four components found at 4.2 K transformed to a doublet at room temperature, the other three sextets merged into a broad distribution. (Ref. 36)
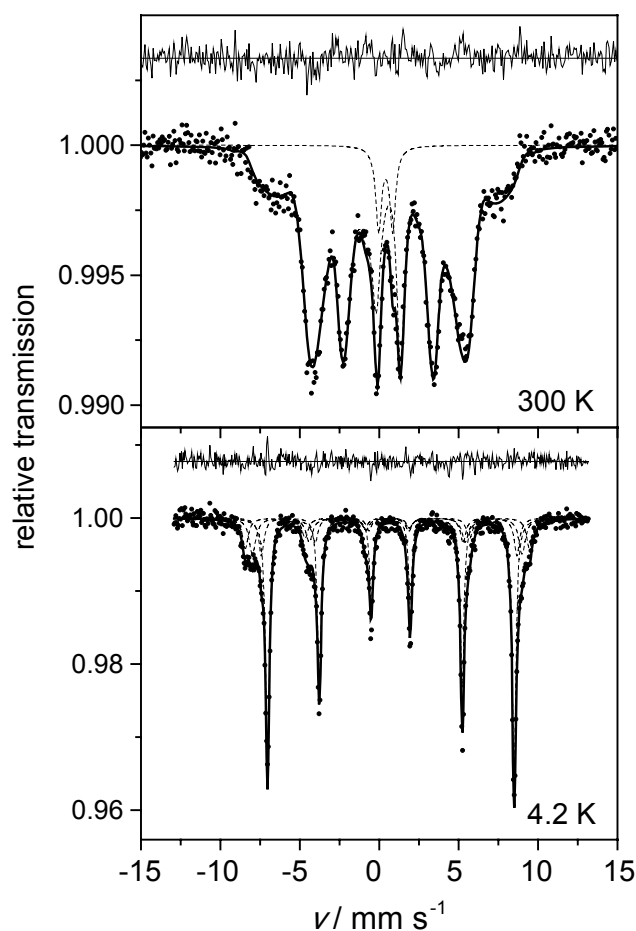
structure and physicochemical properties of double perovskites are then controlled by the size and valences of the different cations. From the magnetic point of view, double perovskites exhibit a variety of magnetic regimes, a result of the numerous ferromagnetic and antiferromagnetic interactions between nearest-neighbor and next-nearest-neighbor cations. Sr_2FeMO_6 (M = Mo, Re, Ru etc.) double perovskites and their doped derivatives have usually high magnetic ordering temperatures and consequently high tunneling type magnetoresistance values even at room temperature (see e.g. Figure 4),[8,21-27] making them potential candidates for next generation MR devices. On the way to explore the source of magnetoresistance of these systems, intensive research was conducted on several member of this family of compounds. As one of the significant results, cation disorder and the resulting nanometer scale electronic phase separation were explained as the possible source of the unusually strong magnetoresistance.[28-31] However, it was also suggested that the TMR effect of double perovskites measured with low external magnetic fields originates from the tunneling of electrons through the grain boundaries.[22] Anyhow, Chamissem et al have found two iron components in Sr_2FeMoO_6, one with the expected 6 Mo neighbors, maintaining strong electron delocalization between Fe and Mo, and one with a lower degree of delocalization. 30% of the iron ions belonged to the latter type, and they were attributed being next to Mo vacancies.[32] This effect was modeled successfully with the help of Mössbauer investigations.[33] It seemed to be interesting to investigate these double perovskites focusing on the occurrence of nanosize phase separation.

Effect of cation disorder. Sr_2FeMoO_6 has been known as a conducting ferrimagnet with a relatively high magnetic transition temperature of $T_C \approx 410$ K.[34] Recently, however, neutron diffraction measurements revealed zero magnetic moment on Mo cations, and consequently the ferrimagnetic structure of Sr_2FeMoO_6 was disputed.[35] It was suggested that while localized magnetic moment can be found only on ferromagnetically arranged Fe^{3+} cations, the $4d^1$ electron of Mo is delocalized as well as spin polarized due to the involvement of Fe^{3+} t_{2g} levels in the conduction band, the latter being formed by the hybridization of 3d (Fe) and 4d (Mo) electronic states.[35-37] Inspired by the high ratio of the second iron component (corresponding to disordered iron cations),[32] we prepared a Sr_2FeMoO_6 sample with higher cation disorder in order to examine the expected local separation of phases via the different iron environments.

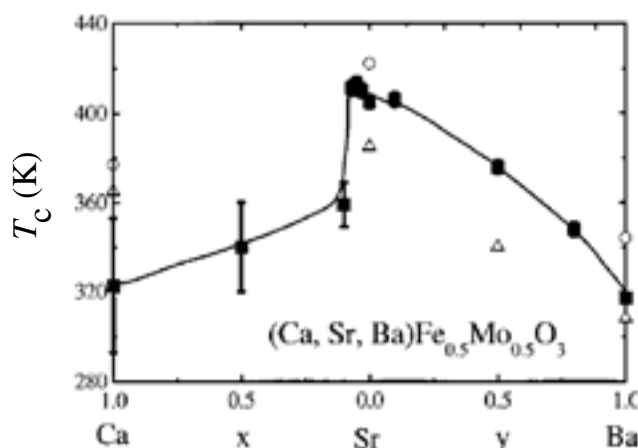The temperature and frequency dependence of the real com-

ponent (χ') in AC susceptibility of the Sr_2FeMoO_6 sample with high cation disorder indicates spin glass or spin cluster glass-like behavior with a glass transition temperature above the highest temperatures used (Figure 5).[38] Figure 6 shows the ^{57}Fe Mössbauer spectra of Sr_2FeMoO_6 measured at T = 300 K and 4.2 K.[38] The latter can be decomposed into four different magnetically split subspectra reflecting magnetically ordered iron cations with different electronic configurations on the 3d level. It was shown, that the two major components reflect iron ions in the ideal, perfectly ordered regions of the double perovskite (showing a high degree of hybridization between 3d(Fe) and
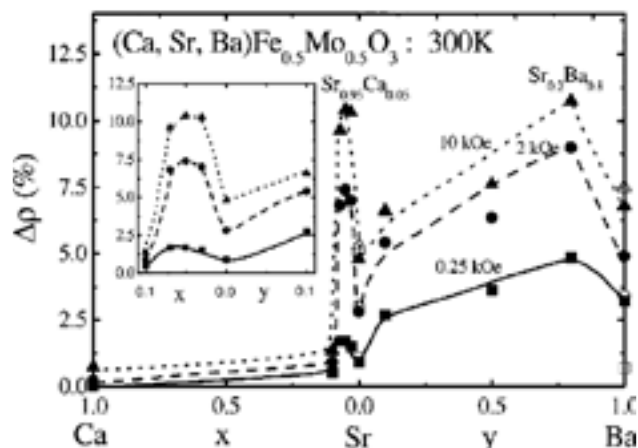
Figure 7. The change of room temperature magnetoresistance of $Sr_{2-x-y}Ba_yCa_xFeMoO_6$ due to Ba or Ca doping (*y* and *x*, respectively) measured with the indicated external magnetic fields. (Ref. 39)

Figure 9. [57]Fe Mössbauer spectra (left panel) of $Sr_{2-x}Ba_xFeMoO_6$ ($0 \leq x \leq 2$) at room temperature and the corresponding distributions of the hyperfine magnetic fields of the major component. a)–f) represent $x = 0, 0.2, 0.4, 1, 1.8$, and 2, respectively.

Figure 8. The change of Curie-temperature of $Sr_{2-x-y}Ba_yCa_xFeMoO_6$ with Ba or Ca doping (*y* and *x*, respectively). (Ref. 39)

4d(Mo) electronic levels) and one with decreased electron density at the minority spin $3d^{5+\delta}$ level of iron, respectively.[32] The decreased minority spin electron density can be interpreted as a reduced degree of delocalization of the $4d^1$ electron of Mo ions. The two extra subspectra with lower isomer shifts and higher hyperfine magnetic fields refer to iron ions in strongly disordered regions of the studied sample, where the delocalization of Mo electrons is suppressed.[38] Increasing the temperature of the sample, one observes a considerable broadening of the absorption lines (Figure 6), implying that with the higher mobility of electrons, due to the increasing thermal energy, a distribution in the level of electron-delocalization develops. In overall, the evaluation of the Mössbauer spectra was in a very good accordance with the theory of small size phase separation, occurring due to the cation disorder in Sr_2FeMoO_6 double perovskite.

Effect of doping on Sr site. Doping Sr_2FeMoO_6 with a small amount of Ba or Ca on the Sr sites increases the magnitude of magnetoresistance significantly.[39] It was shown that room temperature MR doubled when 5% of strontium was exchanged to Ca or when 80% of strontium was replaced by Ba ions (Figure 7) along with the change of the Curie-temperature (Figure 8). These phenomena were explained by the chemical pressure effect of doping, as the major source of MR in these double perovskites is associated with the tunneling of polarized electrons.[39] Our recent [57]Fe Mössbauer study of Ca and Ba doped Sr_2FeMoO_6 double perovskite has shown that Ba doping increases the isomer shift of the main component (being a
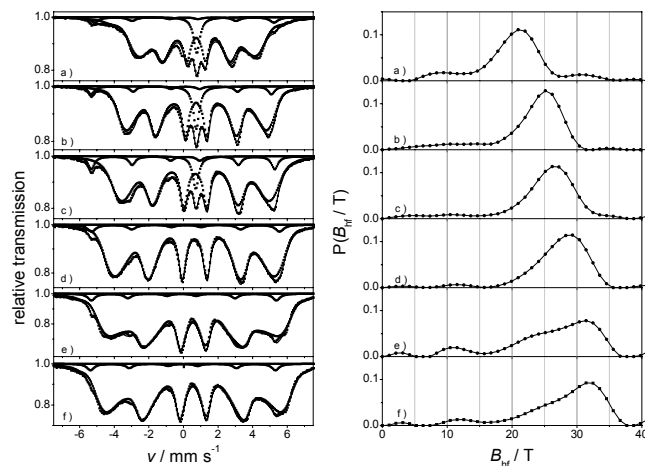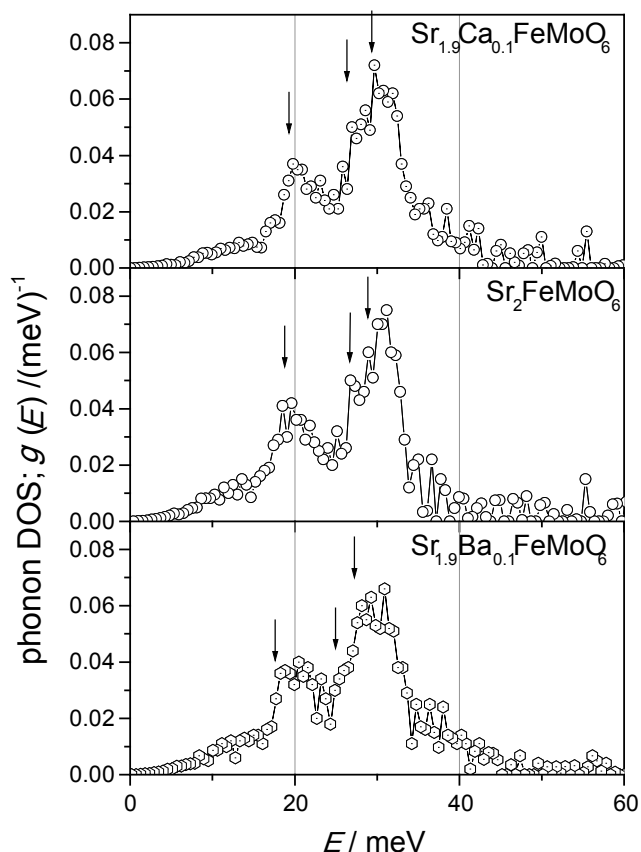
broad sextet, best fitted with a distribution of magnetic hyperfine field) and decreases the maximal magnetic field (Figure 9).[40] These indicate clearly the decreased level of hybridization between Mo and Fe atoms occurring due to increasing the Ba content. While the root of this phenomenon lies in the different cationic size of Sr and Ba ions and thus in the change of lattice parameters (often called as chemical pressure), the result is a higher electric resistance and a lower T_C. Besides, it was found that chemical pressure affects the phonon DOS (density of states), determined by nuclear inelastic scattering, of 5% Ba and Ca doped Sr_2FeMoO_6, too.[40] While in the case of Ba doping the phonon peak edges shifted to lower energies, indicating softening of the lattice due to the expansion of the lattice cell, Ca doping result shows the opposite tendency (Figure 10).

On the other hand, in the Re based analogue, Sr_2FeReO_6 resistivity and Curie temperature increases with Ca doping as a consequence of changing the level of hybridization of Fe 3d and Re 5d electrons.[41] The strong hybridization between Fe and Re was shown in many studies, and a model for cation disorder was stated.[42,43] Investigating the effect of Ba doping at the crystallographic site of Sr in $Sr_{2-x}Ba_xFeReO_6$ double perovskites with $x = 0$ and 0.1, three iron components were found due to cation disorder (Figure 11).[44] Although the saturation magnetization of Sr_2FeReO_6 was drastically decreased by the introduction of $x = 0.1$ barium ions (Figure 12), the hyperfine parameters obtained from the Mössbauer spectra at low temperatures show only slight changes. However, above the magnetic transition temperature the observed intensity ratio of the singlet and the doublet, associated with the ordered iron ions with 6 Re neighbors and the disordered iron ions, respectively, is surprisingly low. This phenomenon was explained by the low crystalline size of the samples (being between 80 nm and 800 nm) due to the sol-gel preparation, resulting in a higher number of disordered iron ions.[44] Moreover, significant dependence of the Mössbauer-Lamb factor for the different iron species was also pointed out, which contributed to the low area ratio of the singlet subspectrum.[44] These results suggest that in samples prepared to have small crystalline size the ratio of disordered and ordered regions can be tuned in a great extent, resulting in significant changes of bulk magnetic properties and so of their magnetotransport.

The cobalt based double perovskite, $Sr_2FeCoO_{6-\delta}$, has a spin-polarized conduction band similar to that of the Sr_2FeMoO_6 relatives, the former having Co^{4+}/Co^{3+} ion pairs with itinerant electron holes instead of Mo^{5+}/Mo^{6+} with itinerant electrons on the t_{2g} level.[45,46] Both materials show no sign of either Jahn-

Mössbauer studies for exploring CMR and TMR perovskites

J. Nucl. Radiochem. Sci., Vol. 9, No. 2, 2008 **R5**
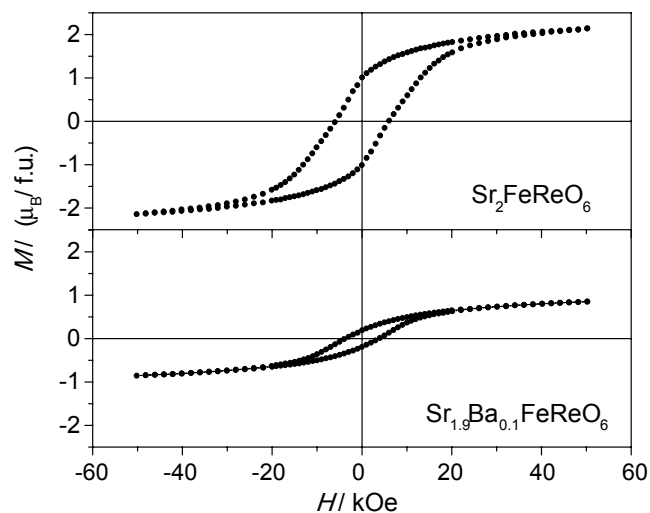

Figure 10. Phonon DOS distributions of undoped and 5% Ca or Ba doped Sr_2FeMoO_6 double perovskite measured by nuclear inelastic scattering.
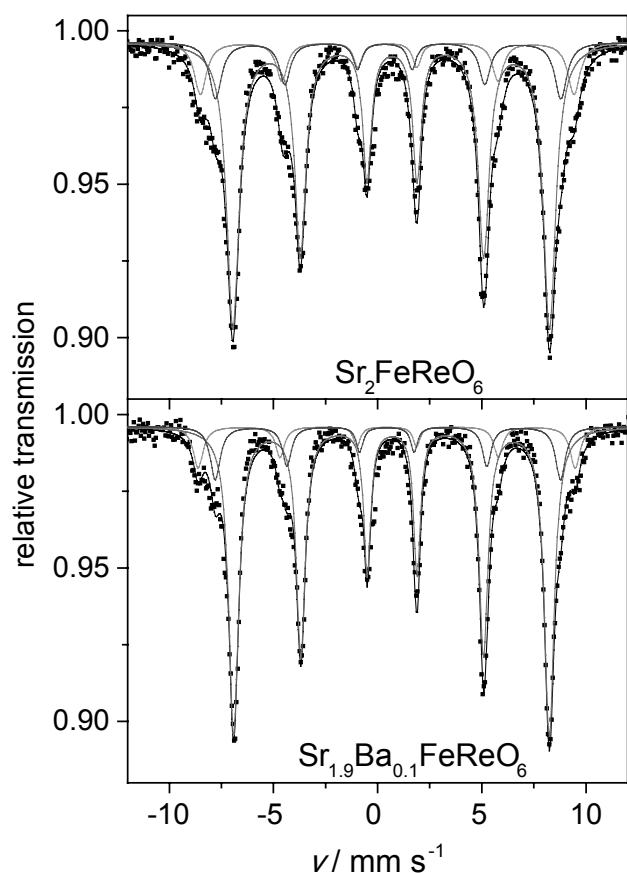
Figure 11. ^{57}Fe Mössbauer spectra of Sr_2FeReO_6 (top) and $Sr_{1.9}Ba_{0.1}FeReO_6$ (bottom) double perovskites at 10 K.

Figure 12. Magnetic hysteresis curves of Sr_2FeReO_6 (top) and $Sr_{1.9}Ba_{0.1}FeReO_6$ (bottom) measured at 10 K.

tronic structure of double perovskites to understand the basic roots of their MR. The study of these perovskites with the resonant nuclear inelastic scattering method revealed significant changes in the phonon spectra of iron at the magnetic ordering temperature ($T_C \approx 150$ K), such as narrowing and softening of the low energy peaks near 12–14 meV, which are well separated from the main energy bands at 20–45 meV. The latter softens below T_C, too, which feature was attributed to the effect of the lattice vibrations on the formation of the spin-polarized band.[49]

Recently, ruthenium based double perovskites became extensively studied due to their rich magnetic phase diagram and various magnetic exchange interactions. As the most popular example, $CaRuO_3$ and $SrRuO_3$ perovskites revealed similar chemical and structural properties, although their magnetic characteristics differ significantly.[50-56] While $SrRuO_3$ is a ferromagnet with $T_C = 160$ K, $CaRuO_3$ is a spin glass with short range antiferromagnetic interactions. $Ca_xSr_{1-x}RuO_3$ ruthenates show a gradual transition between the magnetic states of the two extreme compositions.[57-60] As for the Fe-rich, Sr_2FeRuO_6 ruthenate, beside its TMR effect[59] it indicates a high degree of Fe/Ru disorder and spin-glass structure at 4.2 K as reflected through the wide distributions of the hyperfine interactions in ^{57}Fe Mössbauer spectra.[61] Later on, the spin-glass behavior of Sr_2FeRuO_6 was proved by combined magnetic and Mössbauer data and simulation studies, too, with a transition temperature of 60 K.[62-64] We have studied the effect of cation substitution at the strontium site of Sr_2FeRuO_6 double perovskite, too. According to the transmission electron microscopic and scanning electron microscopic studies, the average particle size of the samples produced (Sr_2FeRuO_6, $Sr_{1.9}Ba_{0.1}FeRuO_6$, and $Sr_{1.9}Ca_{0.1}FeRuO_6$) were between 15 nm and 70 nm, as a consequence of the sol-gel preparation method.[65] The small level of doping resulted in very small changes in the cell parameters for both Ca and Ba, but they altered the local and bulk magnetic properties considerably. Magnetization and in-field Mössbauer spectroscopy measurements fortified the spin glass state below the magnetic transition temperature for these materials, the magnetic freezing point being 64 K, 66 K, and 86 K for the calcium, barium, and undoped sample, respectively.[65] Moreover, Ca doping was found to strengthen the antiferromagnetic interactions, as the Weiss temperature was found to be more negative with about 50 K in $Sr_{1.9}Ca_{0.1}FeRuO_6$ than in the parent Sr_2FeRuO_6.[65] This shows again that doping the strontium site with different sized divalent cations affects long range magnetic interactions in a great extent. That is, the magnetic properties and so the magnetoresistance of double

Teller distortions or double exchange effects.[47] However, their high magnetoresistance[48] urged for a detailed study of the elec-

perovskites can be tuned effectively with optimizing the composition.

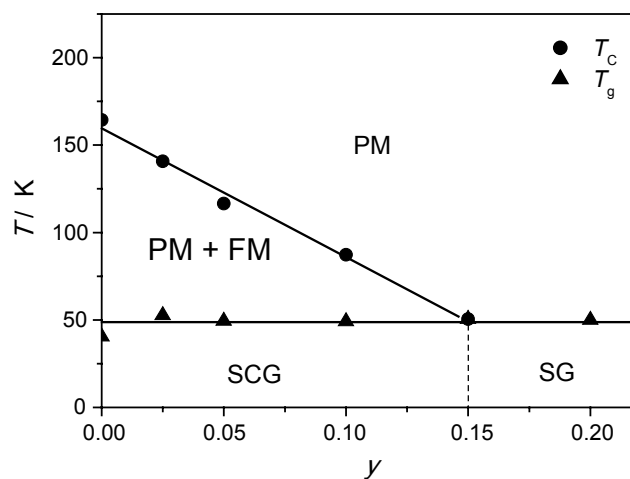## 3. $La_{0.8}Sr_{0.2}Fe_yCo_{1-y}O_{3-\delta}$ perovskites with $0 \leq y \leq 0.3$

In the case of the $LaCoO_3$ derived perovskites, doping with divalent ions (e.g. Ca, Sr) at the rare-earth site results in converting some Co^{3+} ions into Co^{4+} (and thus introducing electron holes in the transition metal network) as well as increasing the average spin state of cobalt ions.[12] Strontium substitution also alters the electronic transport, the magnetic, as well as the MR properties of these materials.[9-12,66-74] While $La_{1-x}Sr_xCoO_{3-\delta}$ is a semiconductor for low Sr concentration levels, it becomes ferromagnetic as well as metallic above $x \geq 0.18$ strontium doping. Below the doping level $x = 0.18$ $La_{1-x}Sr_xCoO_{3-\delta}$ shows semiconducting characteristics accompanied by only short range magnetic correlations with a characteristic coherence length of a few nanometers. Below ~ 60 K the magnetization of these separate magnetic droplets freezes out to some locally preferred direction, and the material enters a glassy magnetic state. Above $x \approx 0.18$, below the Curie temperature coalesced ferromagnetic clusters coexist with insulating, magnetically disordered regions on the nanometer scale. The magnetic clusters are thought to owe their ferromagnetic and metallic character to the double exchange effect between Co^{3+} and Co^{4+}. At the same time, in the insulating regions superexchange interaction between nearest neighbor Co^{3+} ions is thought to be responsible for the absence of long-range ferromagnetic order and diminished electrical conductivity. The simultaneous presence of ferromagnetic (between Co^{4+} and Co^{3+}) and antiferromagnetic (between Co^{3+} and Co^{3+}) exchange interactions, as well as the possible occurrence of Co in a diamagnetic (low-spin Co^{3+}) state, leads to the formation of a glassy magnetic state, which visualizes itself as a spin-glass (for $x \leq 0.18$) or as a cluster-glass (for $x > 0.18$).[12,75]

Magnetoresistance of $La_{1-x}Sr_xCoO_{3-\delta}$ depends strongly on the doping level x. While for $x \geq 0.2$ a CMR peak around T_C is dominant, for $x \leq 0.18$ tunneling-like magnetoresistance is most pronounced at low temperatures below the spin-glass freezing temperature (this behavior is sometimes referred to as 'low-T MR'). For $0.18 \leq x \leq 0.2$ the two types of MR occur simultaneously.

Doping of $La_{1-x}Sr_xCoO_{3-\delta}$ at the transition metal site with iron (resulting in $La_{1-x}Sr_xFe_yCo_{1-y}O_{3-\delta}$ perovskites) considerably enhances low-T magnetoresistance,[76,77] while at the same time also reversing the effect of Sr doping from the viewpoint of bulk magnetization and electrical conductivity, and also it was suggested that the alteration of the MR properties of the investigated iron doped cobalt perovskites can be interpreted by the modification of the magnetic field induced low-spin to high-spin transition of Co^{3+} ions.[77] However, the effect of iron doping on cobaltate perovskites on the local and bulk electronic and magnetic properties was far from being explored or understood.

We carried out measurements on members of the $La_{1-x}Sr_xFe_yCo_{1-y}O_{3-\delta}$ family of compounds with the aim to explore the local electronic and magnetic structure of these perovskites around the magnetic phase transition regime ($x \approx 0.2$).

Figure 13 shows the magnetic phase diagram of $La_{0.8}Sr_{0.2}Fe_yCo_{1-y}O_{3-\delta}$ ($0 \leq y \leq 0.2$) perovskites, as suggested by magnetic susceptibility measurements (Figure 14) and ^{57}Fe Mössbauer spectroscopy (Figure 15 and Figure 16).[78-81] Ferromagnetism, i.e. the presence of magnetically ordered clusters displaying a substantial effective magnetic moment and a characteristic size well above ~ 10 nm, is observed only for $y < 0.15$, but even in this iron concentration range paramagnetic (as well as superparamagnetic) regions coexist with the magnetically ordered ones (Figure 13). As referred to also by the temperature dependence of the in-phase part of the AC magnetic susceptibility

Figure 13. Magnetic phase diagram of $La_{0.8}Sr_{0.2}Fe_yCo_{1-y}O_{3-\delta}$ ($0 \leq y \leq 0.3$) perovskites. PM denotes paramagnetic, FM ferromagnetic, SCG spin-cluster glass, while SG spin-glass phases.
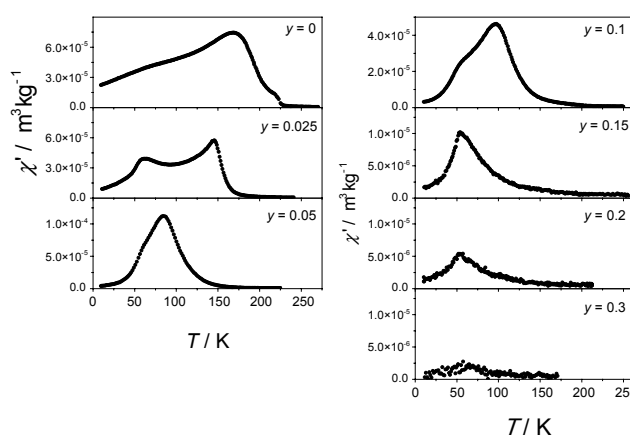
**Figure 14.** Real part of AC magnetic susceptibility of $La_{0.8}Sr_{0.2}Fe_yCo_{1-y}O_{3-\delta}$ ($0 \leq y \leq 0.3$) perovskites as a function of temperature.
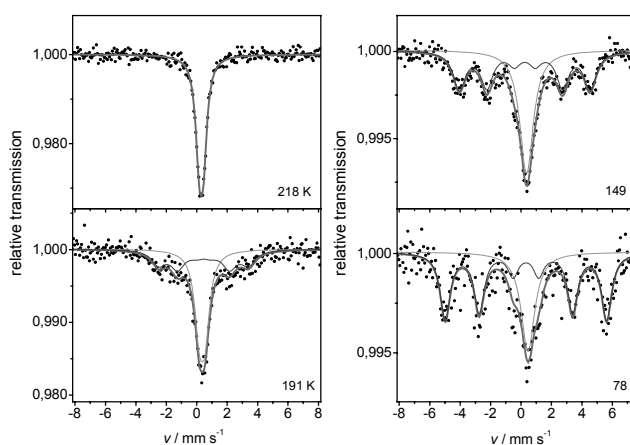
Figure 15. ^{57}Co emission Mössbauer spectra of $La_{0.8}Sr_{0.2}CoO_{3-\delta}$ measured at the temperatures indicated.

(Figure 14), magnetic glass-freezing transition was observed in all the studied samples ($y \leq 0.3$): below $T_g \approx 53$ K the magnetic state of $La_{0.8}Sr_{0.2}Fe_yCo_{1-y}O_{3-\delta}$ ($y \leq 0.3$) resembles that of a spin-glass (for $y \geq 0.15$) or spin-cluster glass (for $y < 0.15$). Interestingly, the temperature at which this glass-freezing transition occurs does not seem to depend on the iron concentration y.

The magnitude of χ' shows a decreasing tendency with increasing iron concentration (Figure 14), showing that iron substitution gradually suppresses ferromagnetic correlations.
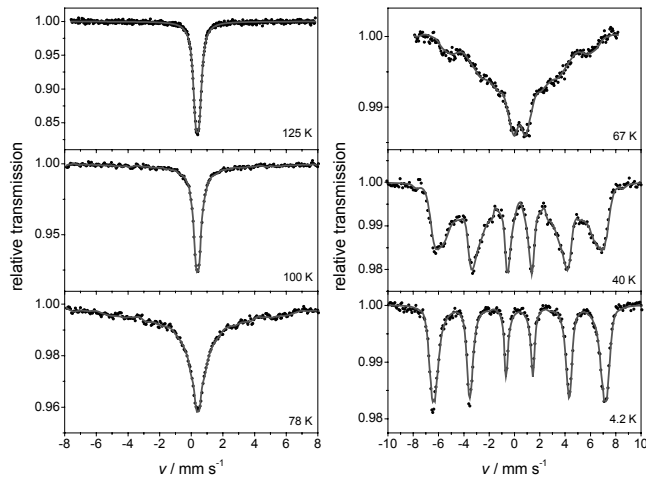
Figure 16. ^{57}Fe Mössbauer spectra of $La_{0.8}Sr_{0.2}{}^{57}Fe_{0.05}Co_{0.95}O_{3-\delta}$ measured at the temperatures indicated.

Figure 17. ^{57}Fe Mössbauer isomer shifts of $La_{0.8}Sr_{0.2}Fe_yCo_{1-y}O_{3-\delta}$ ($y \leq$ 0.025) as a function of temperature.

Figure 18. Temperature dependence of the magnetoresistive property of $La_{0.8}Sr_{0.2}Fe_yCo_{1-y}O_{3-\delta}$ ($0 \leq y \leq 0.3$) perovskites.

Indeed, comparing to the Curie temperature value of $La_{0.8}Sr_{0.2}CoO_{3-\delta}$ (being T_C = 220 K), for the sample with y = 0.05 (by applying the Curie-Weiss formula for the high temperature part, T > 185 K, of the AC susceptibility) T_C = 120 K can be identified as Curie temperature, along with 3.2 μ_B/f.u. effective magnetic moment.[80] In contrast, the in-phase part of AC magnetic susceptibility displays no ferromagnetic transition for $La_{0.8}Sr_{0.2}Co_{1-y}Fe_yO_3$ with $y \geq 0.15$.[81] However, as the temperature dependence of the inverse of χ' revealed,[81] above the glass-freezing temperature the seemingly paramagnetic state consists of magnetically ordered atom clusters in which the magnetic moment of a substantial fraction of magnetic ions is oriented opposite to that of the cluster, which in turn results in clusters with a rather small effective magnetic moment. The formation of this state is thought to be mediated by the strong antiferromagnetic exchange interaction between nearest neighbor Fe^{3+} – Fe^{3+} ion pairs, which are expected to be rather abundantly present in the samples with $y \geq 0.15$.

In the samples with low ($y \leq 0.025$) Fe concentrations iron may also be regarded as a probe of the magnetic structure of the host material (i.e. $La_{0.8}Sr_{0.2}CoO_{3-\delta}$): while above the Curie temperature of the ferromagnetic cobalt clusters only a paramagnetic signal can be seen in the corresponding Mössbauer spectra, indicating paramagnetic nucleogenic (in the case of ^{57}Co doping) or aboriginal (in the case of y > 0) Fe^{3+} ions, the spectra measured below T_C show a magnetic subspectrum in addition to the existing paramagnetic doublet (Figure 15). Whereas the magnetic subspectrum can be identified as originating from iron ions connected by magnetic exchange interaction to Co ions in hole-rich clusters of $La_{0.8}Sr_{0.2}CoO_{3-\delta}$, the paramagnetic component signalize the presence of iron in hole-poor paramagnetic regions. In the case of $La_{0.8}Sr_{0.2}{}^{57}Fe_{0.05}Co_{0.95}O_{3-\delta}$ iron doping already results in a substantially decreased Curie temperature[78] as well as in a fragmentation of the ferromagnetic regions into nanosized clusters, which latter is visualized in the ^{57}Fe Mössbauer spectra as a magnetic relaxation effect (most apparent at around 70 K, see Figure 16). For 0.15 $\leq y \leq$ 0.3 $La_{0.8}Sr_{0.2}Fe_yCo_{1-y}O_{3-\delta}$ magnetic relaxation signalizes the formation of the glassy magnetic state by becoming apparent just above the magnetic freezing temperature T_g.[80]

The Mössbauer isomer shifts of the sextets (δ_s) and doublets (δ_d) differ explicitly in each measured spectrum of $La_{0.8}Sr_{0.2}Fe_yCo_{1-y}O_{3-\delta}$ with $y \leq 0.025$: at a given temperature one observes an average gap of about 0.15 mm/s (Figure 17).[79] While the higher δ_d refers to high-spin trivalent state, the lower δ_s values indicate a small decrease of the population of 3d electrons, which can arise from *e.g.* delocalization of valence electrons. This result is in good agreement with the presumption
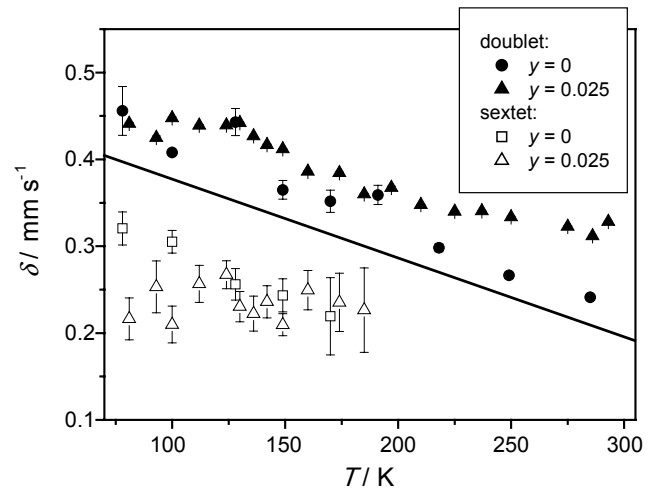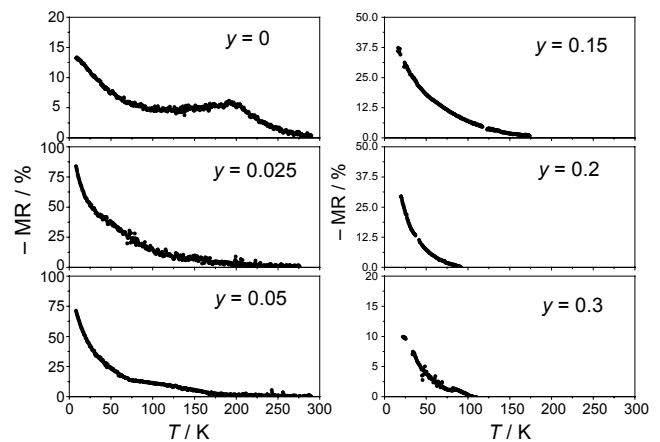
of the cluster model: while in the magnetically ordered conductive clusters the e_g electrons of the Co^{3+} ions are delocalized between the trivalent and tetravalent cobalt ions (due to the double exchange process, resulting in metallic conduction and ferromagnetic exchange interaction), in the paramagnetic matrix they remain more localized. Thus, the isomer shift referring to the ions in the ferromagnetically ordered clusters should be indeed lower (representing a mixed 3+ and 4+ valance character) than that of the doublets referring mostly to the paramagnetic matrix. This finding points out the existence of an electronic phase separation in the aforementioned cobaltate perovskites.

With the help of the electronic phase separation based cluster theory, the observed magnetoresistance (Figure 18)[79] can be explained satisfactorily. As long as the long-range ordered magnetic clusters are maintained ($y \leq 0.05$), a CMR peak around T_C can be seen, as a consequence of the ordering effect an external magnetic field exerts on the magnetic clusters. However, the efficiency of this ordering effect depends on the size, number, and interconnectivity of available clusters, which factors are most sensitive to doping at around the percolation threshold ($x \approx 0.18$). At this threshold the introduction of iron effectively destroys (i.e. frustrates, fragments) larger ferromagnetic clusters as well as their interconnectivity, which results in a suppression of the CMR peak. For $y \geq 0.15$ the clusters become too separated to produce colossal magnetoresistance. On the other hand, the low-temperature magnetoresistance is enhanced drastically with small iron doping (Figure 18). This type of magnetoresistance of cobaltate perovskites is believed

to origin from spin-dependent electron transfer between isolated ferromagnetic clusters, where the external magnetic field orientates the spins of clusters, thus increasing hopping probability. The intensity of the resulting MR, which should depend on the size and distance of clusters, increases with decreasing strontium content in $La_{1-x}Sr_xCoO_{3-\delta}$ perovskites. While the intense growth of MR at low temperatures as a result of $y = 0.025$ iron doping may be explained by a break-up of FM clusters via individual iron ions, the decrease of low-T MR on further increase of y may be connected to the insulating nature of electron paths involving antiferromagnetic $Fe^{3+} - Fe^{3+}$ ion pairs, as well as to the intercluster distances becoming too far for effective electron hopping.

4. Summary

On the search for the roots of strong magnetoresistance in perovskite structured systems, we have traced the occurrence and also the possibility of modulation of electronic and magnetic phase separation, which is thought to be responsible for the realization of both CMR and TMR effects. Our investigations on the local electronic and magnetic state of cobalt based doped CMR perovskites as well as of iron based double perovskites showing TMR effect fortify the presence of coexisting nanometer scale magnetic phases. It seems that the easiest and most reasonable way to improve magnetoresistance in these materials is the accurate adjustment of the composition with a distinguished attention on the small amount of doping cations. With the fine alteration of dopants both the local magnetic interactions and the size and interconnectivity of magnetic clusters can be optimized to give maximum magnetoresistance. For high CMR effect easily alignable big clusters are necessary which coalesce below T_m, while for high TMR the optimum condition is to have isolated, frustrated magnetic clusters with short intercluster distance.

References

(1) J. Fontcuberta, Phys. World **12**, 33 (1999).
(2) E. Dagotto, T. Hotta, and A. Moreo, Phys. Rep. **344**, 1 (2001).
(3) E. L. Nagaev, Phys. Rep. **346**, 387 (2001).
(4) R. M. Kusters, J. Singleton, D. A. Keen, R. McGreevy, and W. Hayes, Physica B **155**, 362 (1989).
(5) R. von Helmolt, J. Wecker, B. Holzapfel, L. Schultz, and K. Samwer, Phys. Rev. Lett. **71**, 2331 (1993).
(6) P. Schiffer, A. P. Ramirez, W. Bao, and S-W. Cheong, Phys. Rev. Lett. **75**, 3336 (1995).
(7) K. H. Ahn, X. W. Wu, K. Liu, and C. L. Chien, Phys. Rev. B **54**, 15299 (1996).
(8) K. -I. Kobayashi, T. Kimura, H. Sawada, K. Terakura, and Y. Tokura, Nature **395**, 677 (1998).
(9) V. Golovanov, L. Mihály, and A. R. Moodenbaugh, Phys. Rev. B **53**, 8207 (1996).
(10) R. Mahendiran and A. K. Raychaudhuri, Phys. Rev. B **54**, 16044 (1996).
(11) S. Yamaguchi, H. Taniguchi, H. Takagi, T. Arima, and Y. Tokura, J. Phys. Soc. Jpn. **64**, 1885 (1995).
(12) J. Wu and C. Leighton, Phys. Rev. B **67**, 174408 (2003).
(13) C. Zener, Phys. Rev. **82**, 403 (1951).
(14) A. J. Millis, Nature **392**, 147 (1998).
(15) S. Zhang and Z. Yang, J. Appl. Phys. **79**, 7398 (1996).
(16) J. M. Teresa, M. R. Ibarra, P. A. Algarabel, C. Ritter, C. Marquina, J. Blasco, J. Garcia, A. del Moral, and Z. Arnold, Nature **386**, 256 (1997).
(17) L. M. Rodriguez-Martinez and J. P. Attfield, Phys. Rev. B **54**, R15622 (1996).
(18) M. Uehara, S. Mori, C.H. Chen, and S.-W. Cheong, Nature **399**, 560 (1999).
(19) A. Moreo, M. Mayr, A. Feiguin, S. Yunoki, and E. Dagotto, Phys. Rev. Lett. **84**, 5568 (2000).
(20) Y. Motome and N. Furukawa, Phys. Rev. B **71**, 014446 (2005).
(21) R. D. Sánchez, D. Niebieskikwiat, A. Caneiro, L. Morales, M. Vásquez-Mansilla, F. Rivadulla, and L. E. Hueso, J. Magn. Magn. Mater. **226-230**, 895 (2001).
(22) T. H. Kim, M. Uehara, S-W. Cheong, and S. Lee, Appl. Phys. Lett. **74**, 1737 (1999).
(23) T. Manako, M. Izumi, Y. Konishi, K. -I. Kobayashi, M. Kawasaki, and Y. Tokura, Appl. Phys. Lett. **74**, 2215 (1999).
(24) J. Lindén, T. Yamamoto, J. Nakamura, M. Karppinen, and H. Yamauchi, Appl. Phys. Lett. **78**, 2736 (2001).
(25) J. Lindén, T. Yamamoto, J. Nakamura, H. Yamauchi, and M. Karppinen, Phys. Rev. B **66**, 184408 (2002).
(26) K. -I. Kobayashi, T. Kimura, Y. Tomioka, H. Sawada, K. Terakura, and Y. Tokura, Phys. Rev. B **59**, 11159 (1999).
(27) J.H. Kim, G. Y. Ahn, S-I Park, and C. S. Kim, J. Magn. Magn. Mater. **282**, 295 (2004).
(28) L. Pinsard-Gaudart, R. Surynarayanan, and A. Revcolevschi, J. Appl. Phys. **87**, 7118 (2000).
(29) M. García-Hernández, J. L. Martínez, M. J. Martínez-Lope, M. T. Casais, and J. A. Alonso, Phys. Rev. Lett. **86**, 2443 (2001).
(30) T. Saha-Dasgupta and D. D. Sarma, Phys. Rev. B **64**, 064408 (2001).
(31) M. Lü, J. Li, X. Hao, Z. Yang, D. Zhou, and J. Meng, J. Phys.: Condens. Matter **20**, 175213 (2008).
(32) O. Chmaissem, R. Kruk, B. Dabrowski, D. E. Brown, X. Xiong, S. Kolesnik, J. D. Jorgensen, and C. W. Kimball, Phys. Rev. B **62(21)**, 14197 (2000) .
(33) J. M. Greneche, M. Venkatesan, R. Suryanarayanan, and J. M. D. Coey, Phys. Rev. B **63**, 174403 (2001).
(34) T. Nakagawa, J. Phys. Soc. Jpn. **24**, 806 (1968).
(35) B. Garcia-Landa, C. Ritter, M.R. Ibarra, J. Blasco, P.A. Algarabel, R. Mahendiran, and J. Garcia, Solid State Commun. **110**, 435 (1999).
(36) Z. Fang, K. Terakura, and J. Kanamori, Phys. Rev. B **63**, R180407 (2001).
(37) J. Kanamori and K. Terakura, J. Phys. Soc. Jpn. **70**, 1433 (2001).
(38) Z. Klencsár, Z. Németh, A. Vértes, I. Kotsis, M. Nagy, Á. Cziráki, C. Ulhaq-Bouillet, V. Pierron-Bohnes, K. Vad, S. Mészáros, and J. Hakl, J. Magn. Magn. Mater. **281**, 115 (2004).
(39) B-G Kim, Y-S Hor, and S-W. Cheong, Appl. Phys. Lett. **79**, 388 (2001).
(40) K. Nomura, A. Rykov, T. Yokoyama, T. Yamakoshi, M. Katada, T. Mitsui, Z. Homonnay, and A. Vértes, J. Radioanal. Nucl. Chem. **266**, 543 (2005).
(41) T. Alamelu, U. V. Varadaraju, M. Venkatesan, A. P. Douvalis, and J. M. D. Coey, J. Appl. Phys. **91**, 8909 (2002).
(42) J. Gopalakrishnan, A. Chattopadhyay, S. B. Ogale, T. Venkatesan, R. L. Greene, A. J. Millis, K. Ramesha, B. Hannoyer, and G. Marest, Phys. Rev. B **62**, 9538 (2000).
(43) S. Nakamura, M. Tanaka, H. Kato, and Y. Tokura, J. Phys. Soc. Jpn. **72**, 424 (2003).
(44) T. Yamakoshi, K. Nomura, T. Kitamori, J. Shimoyama, Z. Nemeth, and Z. Homonnay, Hyperfine Interact. *in press.*
(45) A. Maignan, C. Martin, N. Nguyen, and B. Raveau, Solid State Sci. **3**, 57 (2001).
(46) D. D. Sarma and S. Ray, Proc. Indian Acad. Sci. Chem.

Sci. **113**, 515 (2001).

(47) M. Abbate, G. Zampieri, J. Okamoto, A. Fujimori, S. Kawasaki, and M. Takano, Phys. Rev. B **65**, 165120 (2002).

(48) T. Ido, Y. Yasui, and M Sato, J. Phys. Soc. Jpn. **72**, 357 (2003).

(49) A. I. Rykov, K. Nomura, Ts. Sawada, T. Mitsui, M. Seto, T. Tamegai, and M. Tokunaga, Phys. Rev. B **68**, 224401 (2003).

(50) J. M. Longo, P. M. Raccah, and J. B. Goodenough, J. Appl. Phys. **39**, 1327 (1968).

(51) A. Callaghan, C. V. Moeller, and R. Ward, Inorg. Chem. **5**, 1572 (1966).

(52) T. Sugiyama and N. Tsuda, J. Phys. Soc. Jpn. **68**, 3980 (1999).

(53) F. M. Da Costa, R. Greatrex, and N. N. Greenwood, J. Solid State Chem. **20**, 381 (1977).

(54) I. Felner, U. Asaf, I. Nowik, and I. Bradaric, Phys. Rev. B **66**, 054418 (2002).

(55) I. Felner, K. Nomura, and I. Nowik, Phys. Rev. B **73**, 064401 (2006).

(56) K. Yoshimura, T. Imai, T. Kiyama, K. R. Thurber, A. W. Hunt, and K. Kosuge, Phys. Rev. Lett. **83**, 4397 (1999).

(57) I. Felner and U. Asaf, Physica B **337**, 310 (2003).

(58) G. Cao, S. McCall, M. Shepard, J. E. Crow, and R. P. Guertin, Phys. Rev. B **56**, 321 (1997).

(59) W. Xia, Q. Zhou, H. Xu, L. Chen, and J. He, Physica B **403**, 2189 (2008).

(60) T. He and R. J. Cava, Phys. Rev. B **63**, 172403 (2001).

(61) I. Nowik and I. Felner, Hyperfine Interact. **156/157**, 195 (2004).

(62) P. D. Battle, T. C. Gibb, C. W. Jones, and F. Studer, J. Solid State Chem. **78**, 281 (1989).

(63) T. C. Gibb, R. Greatrex, N. N. Greenwood, and K. G. Snowdon, J. Solid State Chem. **14**, 193 (1975).

(64) T. C. Gibb, J. Mater. Chem. **15**, 4015 (2005).

(65) K. Nomura, R. Zboril, J. Tucek, W. Kosaka, S. Ohkoshi, and I. Felner, J. Appl. Phys. **102**, 013907 (2007).

(66) A. Mineshige, M. Inaba, T. Yao, Z. Ogumi, K. Kikuchi, and M. Kawase, J. Solid State Chem. **121**, 423 (1996).

(67) A. N. Petrov, O. F. Kononchuk, A. V. Andreev, V. A.

Cherepanov, and P. Kofstad, Solid State Ionics **80**, 189 (1995).

(68) D. Phelan, D. Louca, S. Rosenkranz, S.-H. Lee, Y. Qiu, P. J. Chupas, R. Osborn, H. Zheng, J. F. Mitchell, J. R. D. Copley, J. L. Sarrao, and Y. Moritomo, Phys. Rev. Lett. **96**, 027201 (2006).

(69) M. A. Señaris-Rodriguez and J. B. Goodenough, J. Solid State Chem. **118**, 323 (1995).

(70) Y. Tang, Y. Sun, and Z. Cheng, Phys. Rev. B **73**, 012409 (2006).

(71) J. Wu, J.W. Lynn, C.J. Glinka, J. Burley, H. Zheng, J.F. Mitchell, and C. Leighton, Phys. Rev. Lett. **94**, 037201 (2005).

(72) P.L. Kuhns, M. J. R. Hoch, W.G. Moulton, A. P. Reyes, J. Wu, and C. Leighton, Phys. Rev. Lett. **91**, 127202 (2003).

(73) M. Kopcewicz, D. V. Karpinsky, and I. O. Troyanchuk, J. Phys.: Condens. Matter **17**, 7743 (2005).

(74) H. M. Aarbogh, J. Wu, L. Wang, H. Zheng, J. F. Mitchell, and C. Leigthon, Phys. Rev. B **74**, 134408 (2006).

(75) M. Itoh, I. Natori, S. Kubota, and K. Motoya, J. Phys. Soc. Jpn. **63**, 1486 (1994).

(76) A. Barman, M. Ghosh, S. Biswas, S.K. De, and S. Chatterjee: Appl. Phys. Lett. **71**, 3150 (1997).

(77) Y. Sun, Xiaojun Xu, and Y. Zhang, Phys. Rev. B **62**, 5289 (2000).

(78) Z. Németh, Z. Homonnay, F. Árva, Z. Klencsár, E. Kuzmann, J. Hakl, K. Vad, S. Mészáros, K. Kellner, G. Gritzner, and A. Vértes, J. Radioanal. Nucl. Chem. **271**, 11 (2007).

(79) Z. Németh, Z. Homonnay, F. Árva, Z. Klencsár, E. Kuzmann, A. Vértes, J. Hakl, S. Mészáros, K. Vad, P. F. de Châtel, G. Gritzner, Y. Aoki, H. Konno, and J. M. Greneche, Eur. Phys. J. B **57**, 257 (2007).

(80) Z. Németh, Z. Klencsár, E. Kuzmann, Z. Homonnay, A. Vértes, J.M. Greneche, B. Lackner, K. Kellner, G. Gritzner, J. Hakl, K. Vad, S. Mészáros, and L. Kerekes, Eur. Phys. J. B **43**, 297 (2005).

(81) Z. Klencsár, Z. Németh, E. Kuzmann, Z. Homonnay, A. Vértes, J. Hakl, K. Vad, S. Mészáros, A. Simopoulos, E. Devlin, G. Kallias, J.M. Greneche, Á. Cziráki, and S.K. De, J. Magn. Magn. Mater. **320**, 651 (2008).